**Computers and Concrete**, *Vol. 31, No. 5 (2023) 419-432*
https://doi.org/10.12989/cac.2023.31.5.419



# Nonlinear modeling of beam-column joints in forensic analysis of concrete buildings

Nirmala Suwal[a] and Serhan Guner*

*Department of Civil and Environmental Engineering, The University of Toledo, 2801 W Bancroft St. MS 307, Toledo, Ohio 43607, USA*

(*Received January 5, 2023, Revised March 6, 2023, Accepted March 23, 2023*)

**Abstract.** Beam-column joints are a critical component of reinforced concrete frame structures. They are responsible for transferring forces between adjoining beams and columns while limiting story drifts and maintaining structural integrity. During severe loading, beam-column joints deform significantly, affecting, and sometimes governing, the overall response of frame structures. While most failure modes for beam and column elements are commonly considered in plastic-hinge-based global frame analyses, the beam-column joint failure modes, such as concrete shear and reinforcement bond slip, are frequently omitted. One reason for this is the dearth of published guidance on what type of hinges to use, how to derive the joint hinge properties, and where to place these hinges. Many beam-column joint models are available in literature but their adoption by practicing structural engineers has been limited due to their complex nature and lack of practical application tools. The objective of this study is to provide a comparative review of the available beam-column joint models and present a practical joint modeling approach for integration into commonly used global frame analysis software. The presented modeling approach uses rotational spring models and is capable of modeling both interior and exterior joints with or without transverse reinforcement. A spreadsheet tool is also developed to execute the mathematical calculations and derive the shear stress-strain and moment-rotation curves ready for inputting into the global frame analysis. The application of the approach is presented by modeling a beam column joint specimen which was tested experimentally. Important modeling considerations are also presented to assist practitioners in properly modeling beam-column joints in frame analyses.

**Keywords:** beam-column joint; bond slip; exterior joints; global frame analysis; interior joints; nonlinear analysis; rotational spring; shear

## 1. Introduction

Forensic structural engineering studies structural systems with the objective of identifying the causes of structural failures (e.g., Vecchio *et al*. 2004). A plastic-hinge-based global frame analysis is commonly used in these studies to model the deformations, cracking, and failure modes in reinforced concrete buildings (Parisi and Augenti 2017). One important, and often omitted, aspect of global frame analyses is the modeling of beam-column joints. A beam-column joint (also called a joint core) is where a beam and column intersect in a building frame. While most beam and column failure modes are commonly considered in global frame analyses, the joint failure modes, including concrete shear (see Fig. 1(a)) and reinforcement bond slip (see Fig. 1(b)), are frequently omitted. Experimental studies and post-earthquake inspections have demonstrated that beam-column joints may undergo severe deformation leading to local damage, or, in extreme cases, failures affecting the entire frame structure (Ghobarah and Said 2002, Shin and LaFave 2004, Birely *et al*. 2012). It is, therefore, imperative to model beam-column joints in a global frame analysis, especially for older structures with non-ductile joint designs.

Modeling of beam-column joints can be undertaken using several theoretical approaches with varying degrees of complexity. They range from simple rotational spring models to more elaborate component or finite element models. More recently, machine-learning based models are also proposed. The main phenomena considered in all these joint models are the shear deformation in the joint core due to applied shear forces from columns and beams and the bond slippage of the main reinforcing bars of beams passing through the joint core.

The objective of this study is to provide a comparative review of the available beam-column joint models and present a practical beam-column joint modeling approach for integration into commonly used global frame analysis software. The presented modeling approach uses rotational spring formulations to model both interior and exterior joints with or without transverse reinforcement. The modeling approach is sought to be numerically efficient, readily implementable into global frame analysis software, and sufficiently accurate. The developed spreadsheet tool is intended to assist engineers in deriving the joint hinge properties easily.

*Corresponding author, Professor
E-mail: serhan.guner@utoledo.edu
[a]Graduate Student

## 2. Review of existing beam-column joint models

A significant amount of research has been conducted on


http://www.techno-press.org/?journal=cac&subpage=8

ISSN: 1598-8198 (Print), 1598-818X (Online)

(a) Shear failure mode (Gombosuren and Maki 2020) (b) Bond-slip failure mode (Pantelides *et al.* 2002)

Fig. 1 Beam-column joint primary failure modes

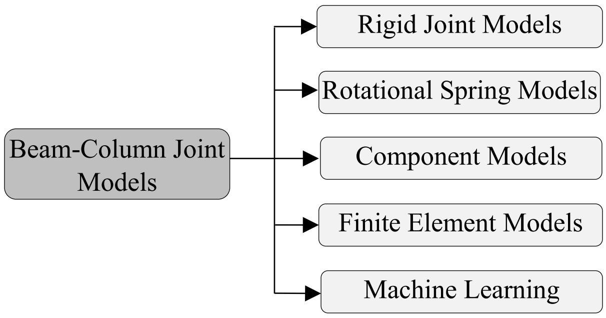


Fig. 2 Classification of beam-column joint models

the nonlinear modeling of beam-column joints. These can be categorized under five distinct types from simple to sophisticated: rigid joint models, rotational spring models, component models, finite element models, and machine learning-based models (see Fig. 2). The main objective of these models is to capture the shear deformation in the joint core and the bond slip of the reinforcing bars.

Subjected to lateral cyclic loading, joint cores experience high shear forces from the adjacent columns and beams. A bending moment applied from each side is carried by a force couple that is formed with tension in the tensile reinforcing bar, and compression in the concrete and the compressive reinforcing bars passing through the joint core. The shear force in the joint core results in shear deformations and the bending moment results in high bond stress between the reinforcing bars and surrounding concrete. The joint response due to shear and bond slip actions may significantly affect the overall stiffness and strength of a frame structure. Most available joint models are, therefore, formulated to capture these two important mechanisms.

### 2.1 Rigid joint models

In the rigid joint models, the beam-column joint core is assumed to be perfectly rigid with no explicit joint modeling undertaken. This model neglects the deformations in the joints and enforces the assumption that the beam and column members remain perpendicular even under significant deformations. Due to the stiffer properties of the joint cores, the nonlinear deformations are concentrated at the ends of the beams and columns, effectively neglecting the joint core behavior. This may result in the overestimation of strength, leading to unsafe designs in terms of ultimate strength and ductility. The predictions of average ultimate strengths that are 86.4% higher than the experimental results are demonstrated in the literature (Sharma *et al.* 2011). This modeling approach may predict the global response of a frame reasonably accurately only if the joints are very well designed and the actual failure mode does not involve any beam-column joint cracking, damage, or nonlinear behavior. For all other cases, this modeling approach is not recommended.

### 2.2 Rotational spring models

Rotational spring models have been used in numerous research studies due to their simplicity and reasonable accuracy. Most rotational spring models introduce rigid link elements and rotational springs in a joint core (see Fig. 3). The rigid link elements simulate the higher strength and stiffness of the joint core (as compared to the adjoining beam and column elements) whereas the rotational spring hinges simulate the shear deformations in the joint core and bond slip behavior at the joint interfaces. The stress-strain or moment-rotation curves are derived, based on various formulations, to define the hinges in rotational spring models. These properties are developed from experimental data calibration based on the joint details and material properties.

Several rotational spring models are available in the literature. Alath and Kunnath (1995) proposed a model, also known as the "scissor model," which models the joints with two components: rigid links and a zero-length rotational spring. The joint core geometry is represented by rigid links while the rotational springs simulate the degrading shear behavior of the joint core. This model accounts only for the shear behavior while the bond slip mechanism is ignored. Biddah and Ghobarah (1999) modified the Alath and Kunnath (1995) model by introducing two separate nonlinear rotational springs in series, one for the joint shear deformation and the other for the bond slip behavior. The Modified Compression Field Theory (MCFT) (Vecchio and Collins 1986) was used to calculate the shear-stress strain relationship. A bilinear idealization of the moment-rotation relationship was used to define the bond slip behavior, capturing critical points such as the cracking, yielding, and ultimate condition.

Park (2010) proposed a semi empirical-analytical model reflecting two key parameters: joint aspect ratio and beam reinforcement index in developing a shear strength model for exterior joints with no transverse reinforcement (non-ductile joint). The shear stress-strain relationship is transformed into a moment-rotation relationship to represent the beam-column joint spring. Sharma *et al.* (2011) proposed a model based on the limiting principal tensile stress theory. They assigned the shear springs to the column region and rotational springs to the beam region within the joint core. This model was developed for only exterior, non-ductile joints with no transverse reinforcement. They validated this model with 12

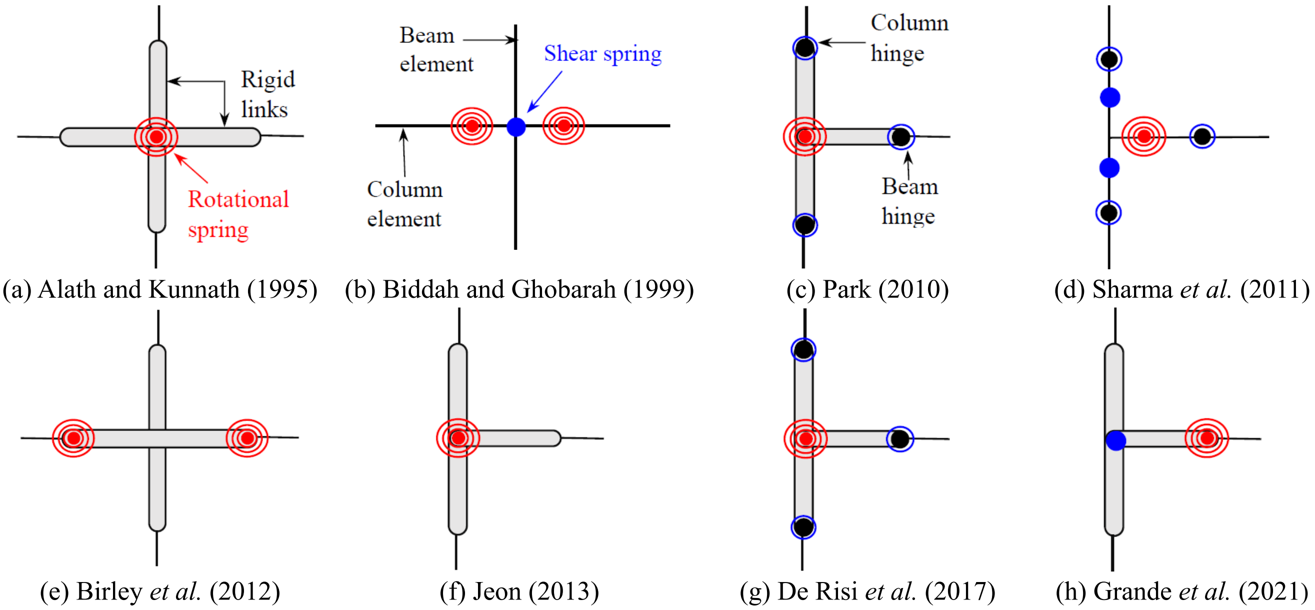


Fig. 3 Mechanical representations of rotational spring models (selected samples)

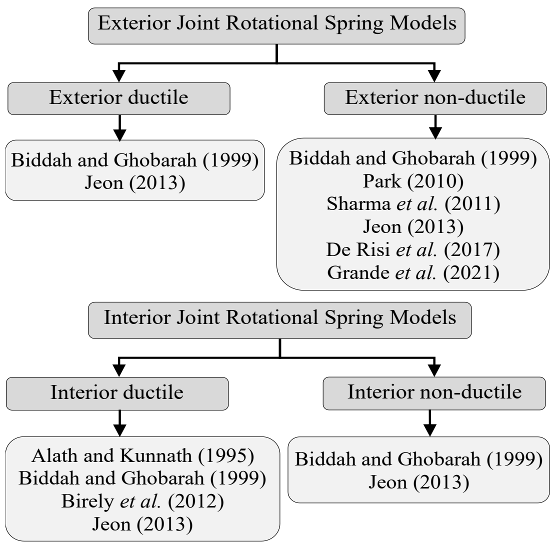


Fig. 4 Rotational spring models (selected samples)

experimental specimens of beam-column joints, with an average error of 8.6%. Birley *et al.* (2012) proposed a model for interior, ductile joints with transverse reinforcement. They used a modified dual-spring in series incorporated in the lumped plastic hinges of the beams. The first spring accounts for the beam response while the second spring captures the joint shear and bond slip responses.

To advance Park (2010), Sharma *et al.* (2011), and Birley *et al.* (2012) models, Jeon (2013) proposed a model that is applicable to the analysis of both exterior and interior joints with and without transverse reinforcement. Jeon (2013) adopted the Alath and Kunnath (1995) model by modifying the joint shear stress-strain curve based on the experimental data from Anderson *et al.* (2008) and utilizing the bond model of Hassan (2011). In addition, Jeon (2013) also proposed an empirical shear strength model to compute the shear strength capacity of joints. Jeon (2013) validated 28 experimental specimens of beam-column joints, with errors up to 8.4%.

De Risi *et al.* (2017) and Grande *et al.* (2021) also adopted the “scissor model” of Alath and Kunnath (1995) with modifications. De Risi *et al.* (2017) calibrated the spring properties based on Celik and Ellingwood (2008) and Jeon (2013) whereas Grande *et al.* (2021) developed a model to compute the shear strength capacity of joints using empirical formulations. Both the De Risi *et al.* (2017) and Grande *et al.* (2021) models are limited to exterior joints without transverse reinforcement.

These rotational spring models are categorized in Fig. 4 according to the joint and ductility types. Ductile joints are typically those with sufficient amounts of transverse reinforcement in the joint core. Non-ductile joints may contain no shear reinforcement, insufficient amounts of shear reinforcement, and/or deficient design detailing. Non-ductile joints exhibit brittle and undesirable failure modes.

### *2.3 Component models*

Component models include sophisticated constitutive models that explicitly model joint core shear and bond slip behaviors. Several component models have been proposed in the literature (see Fig. 5). Many such models use MCFT to determine the shear response of a joint core subjected to shear loads coupled with an axial load. Youssef and Ghobarah (2001), Lowes and Altoontash (2003), and Shin and Lafave (2004) are examples of such models. These studies found that the MCFT underestimates the strength of beam-column joints with low amounts of transverse reinforcement while overestimating it for joints with high amounts of transverse reinforcement. To resolve this, Mitra and Lowes (2007) modified the Lowes and Altoontash (2003) model to broaden the range of applicability while improving the prediction accuracy. They modelled the shear load transfer within a joint core with a diagonal

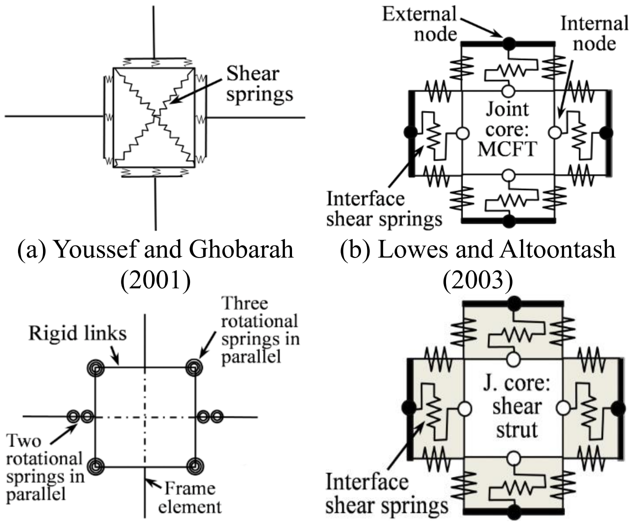


(a) Youssef and Ghobarah (2001) (b) Lowes and Altoontash (2003)

(c) Shin and LaFave (2004) (d) Mitra and Lowes (2007)

Fig. 5 Mechanical representations of component models (selected samples)

compression strut rather than a shear stress field based on the MCFT. They also proposed a new bar-slip model to simulate the frictional resistance of bars combined with hysteretic strength loss.

These studies demonstrate that component models are highly versatile and accurate. However, they require the derivation of multiple constitutive models for the various springs used and are not readily implementable in global frame analysis software using one-dimensional line elements. Therefore, their adoption by practicing structural engineers remains rather limited. In an attempt to make component models more applicable to frame analyses, Pan *et al.* (2017) implemented the Mitra and Lowes (2007) model into a nonlinear distributed-plasticity-based frame analysis procedure, VecTor5 (Guner and Vecchio 2008), for the holistic modeling of frame buildings. They demonstrated practical modeling and successful simulation results based on an experimental validation study of nine specimens.

### *2.4 Finite element models*

Finite element modeling is useful for developing a more comprehensive understanding of the performance of the beam-column joints. Eligehausen *et al.* (2006) utilized continuum finite elements based on microplane model for exterior joints. In this study, the concrete was modelled with an isotropic microplane material, reinforcement with a trilinear steel constitutive law, and the bond between reinforcement and concrete with discrete bond elements. Sharma *et al.* (2009) simulated the behavior of exterior and interior joints using a similar finite element modeling approach. Sagbas *et al*. (2011) modelled beam-column joints using a two-dimensional (2D) continuum element based on secant-stiffness solution algorithm employing a smeared rotating crack model of reinforced concrete (Wong *et al.* 2013). The constitutive modeling of concrete and reinforcement employed the Disturbed Stress Field Model (DSFM) (Vecchio 2000). The bond slip of the longitudinal reinforcement was modelled using discrete truss bars elements. Guner and Vecchio (2011) used a similar theoretical approach in the context of macro 1D elements as a part of a global frame analysis subjected to cyclic load reversals. In this study, beam and column behaviors are also simulated using a distributed inelasticity fiber-section approach. Sasmal and Nath (2016) investigated the crack and failure patterns, shear strengths, cyclic load-displacement behaviors, and energy dissipation and ductility characteristics of several joint specimens using the finite element method. In this study, concrete and reinforcement were modelled as macro-elements - concrete with quadratic brick elements and reinforcement with discrete truss elements. Pan *et al.* (2017) implemented a component joint model into a global nonlinear frame analysis method, VecTor5 (Guner and Vecchio 2008). In this study, both joint shear deformations and bond slip effects were simulated in addition to the nonlinearities in the beams and columns using DSFM (Vecchio 2000). Abusafaqa *et al.* (2022) employed the finite element method to study the effectiveness of ultra-high-performance concrete in beam-column joint strengthening. The concrete was defined with isometric eight node linear brick elements and reinforcement with two-node linear truss elements. The perfect bond was assumed between reinforcement and concrete, neglecting the bond slip behavior. The concrete damage plasticity model was used to simulate the behavior of concrete.

The analysis of beam-column joints using finite element modeling requires significant experience, computational resources, and time. Consequently, this approach is commonly used to simulate the behavior at the local level (i.e., isolated beam-column joints) as opposed to holistic modeling of building frames.

### *2.5 Machine learning models*

Machine learning (ML) is a branch of artificial intelligence (AI) that trains computers to make predictions based on existing datasets and algorithms when fed new data. This approach provides a computational algorithm with the ability to learn and improve until it meets the desired performance rather than explicit coding (Thai 2022). ML models have been increasingly used for predicting the beam-column joint shear strength capacity and failure modes. By utilizing ML, Unal and Burak (2012) created an empirical equation to predict the shear strength capacity of joints. Jeon *et al*. (2014) proposed a joint shear strength model using a multi adaptive regression splines (MARS) algorithm. Kotsovou *et al*. (2017) used an artificial neural network (ANN) to predict the shear strength capacity of the exterior joints. Mangalathu and Jeon (2018) developed expressions to calculate the shear strength capacity and provided formulations to categorize the predicted failure modes. They used the Lasso logistic regression algorithm (Tibshirani 1996). To predict the shear strength capacity and failure mechanisms of exterior joints, Alwanas *et al.* (2019) used an ELM algorithm developed by Huang *et al.* 2006. Naderpour and Mirrashid (2019)

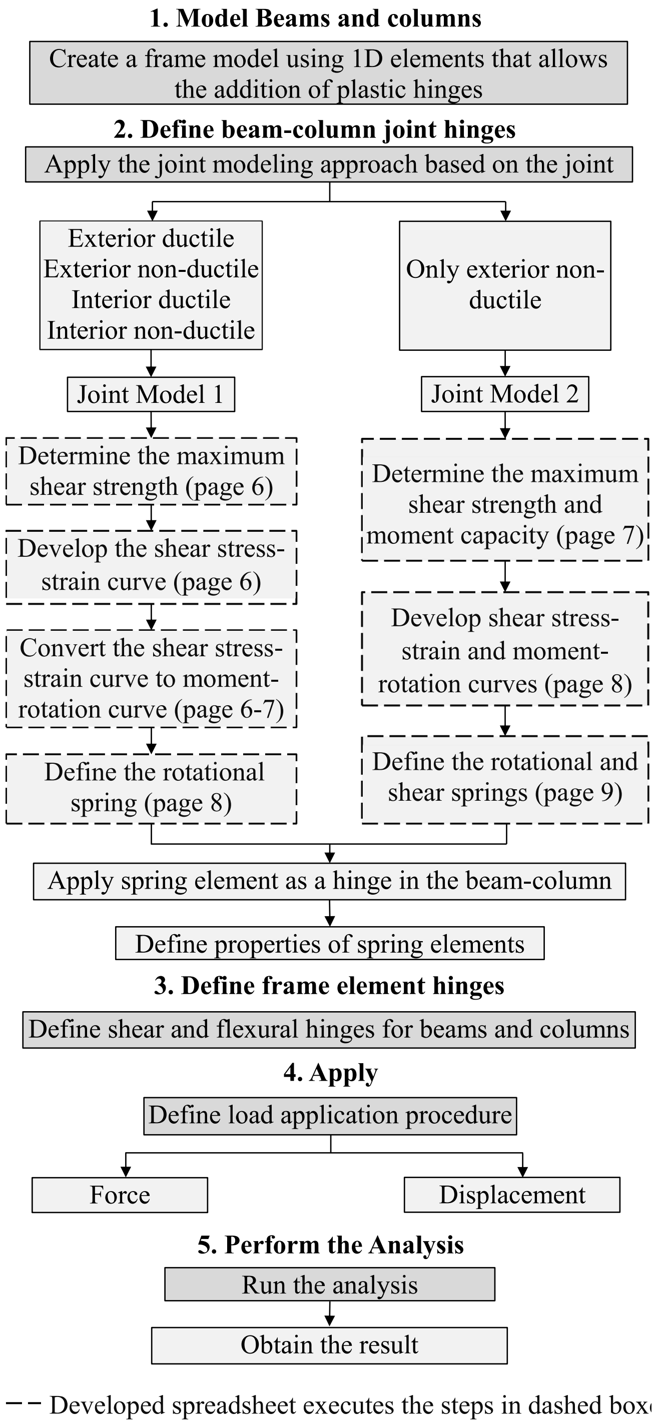


Fig. 6 Flowchart of the proposed joint modeling approach

proposed two failure mode classifiers based on the decision tree method (Wu *et al.* 2008). Gao and Lin (2021) applied ten ML methods to predict the failure modes of beam-column joints. Alagundi and Palanisamy (2022) employed ANNs to predict the shear strengths of exterior joints. Haido (2022) also utilized ANNs to predict the shear strengths of interior and exterior joints and compared the prediction model with alternative approaches contained in the existing building codes.

The analysis of beam-column joints using ML methods is a promising and evolving research field. The studies cited above indicated prediction accuracies as high as those obtained from the physics-based joint models discussed above. One important aspect of ML modeling is that the joint being modelled should be well represented by the dataset used for the development and training.

### *2.6 Discussion*

Among the various types of beam-column joint models available, each model has its own strengths and weaknesses. No scientific consensus has been reached on an optimal model that applies to all cases (Pan *et al.* 2017). Rotational spring models are simple, reasonably accurate, and suitable for practical implementation into global frame analysis software using 1D line elements. Component and finite element models are shown to be more versatile and accurate for a wider range of conditions, but they are computationally demanding and requires significant knowledge and effort from the engineer. Machine learning models provide fast analysis times and promising results. The database selection and the similarity between the dataset and the joint being modelled plays a critical role in their prediction accuracy.

## 3. Proposed beam-column joint modeling approach

As a part of this study, a beam-column joint modeling approach is proposed to aid practicing engineers in incorporating joint modeling into global frame analysis using 1D linear frame elements. The proposed approach integrates rotational spring models (due to their simplicity and reasonable accuracy) into commonly used lumped-plasticity-based frame analysis methods. Fig. 6 shows the overview of the proposed approach.

The first stage is common to any linear-elastic global frame analysis using 1D line elements with a center-line approach; therefore, it is not discussed further. The second stage is to define rotational spring elements as plastic hinges in beam-column joints. Fig. 2 and Fig. 3 show several rotational spring models based on the joint type. The analyst can select any of those models for the nonlinear modeling of the joints. The proposed approach uses two specific beam-column joint models as Model 1 and Model 2. Model 1 provides a wide range of applicability to include exterior, interior, ductile, and non-ductile joints, and is based on Jeon (2013). Model 2 is exclusively for exterior non-ductile beam-column joints which are shown to sustain significant damage due to their brittleness and unbalanced nature (Clyde *et al.* 2000) and is based on Sharma *et al.* (2011).

To model a beam-column joint using Model 1, a rotational spring is introduced at the intersection of beam and column elements (see Fig. 7). The joint core is represented by rigid end offsets due to the overlapping nature of the elements. The inserted rotational spring models the shear and bond slip effects.

To define a rotational spring as a plastic hinge in a global frame analysis, the shear stress-strain curve should

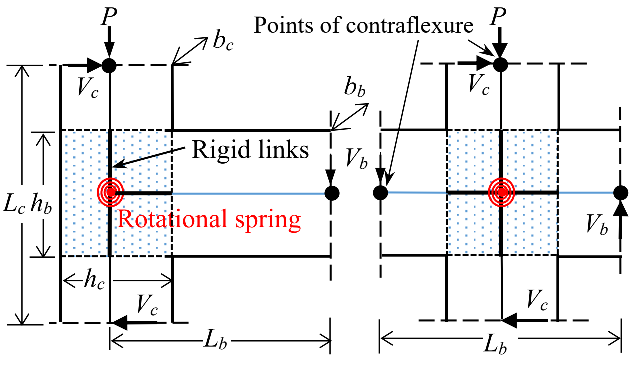


(a) Exterior joint (b) Interior joint

Fig. 7 Location of rotational spring using Model 1

be developed. This curve can be constructed with four points: (1) cracking, (2) yielding, (3) maximum, and (4) residual, where each point is defined as a function of the shear strength ($v_{max}$). The input parameters required to compute $v_{max}$ are the concrete compressive strength ($f'_c$), the cross-sectional dimensions of the beams and columns ($b_b$, $b_c$, $h_b$, $h_c$), the beam length ($L_b$), the axial load factor (ALF), and the reinforcement details. $L_b$ is the length between two points of contraflexure or zero moment as shown in Fig. 7. The ALF is defined as the ratio of the axial load ($P$) to the product of three variables: column gross area ($A_g$), the in-plane geometry factor (1 for interior, 0.75 for exterior, and 0.5 for knee joint), and the transverse beam confinement factor (1 for joints with 0 or 1 transverse beam, and 1.2 for joints with 2 transverse beams). The input parameters related to the reinforcement include the beam longitudinal reinforcement ratio ($\rho_b$), the column longitudinal reinforcement ratio ($\rho_c$), the joint transverse reinforcement ratio ($\rho_{jt}$), the beam longitudinal reinforcement strength ($f_{yb}$), the column longitudinal reinforcement strength ($f_{yc}$), and the joint transverse reinforcement strength ($f_{yjt}$). $V_b$ and $V_c$ are the shear forces in the beams and columns, respectively. To facilitate the calculation process, a spreadsheet tool (Suwal and Guner 2023a) is created for the calculation of $v_{max}$ and shared as a freeware for the use of practicing engineers. A user bulletin (Suwal and Guner 2023b) is also prepared to demonstrate the application and experimental validation of the spreadsheet with four specimens. The sheet employs the calculation process defined in Jeon (2013).

Once $v_{max}$ is computed, the shear stress-strain curve is defined as shown in Fig. 8, where the yield and residual strengths are 95% and 20% of $v_{max}$, respectively. The cracking strength is defined as $0.48\sqrt{f'_c}$. The shear strain ($\gamma$) corresponding to the cracking and yielding strengths are 0.00043 and 0.006, respectively, as adopted from Anderson *et al.* (2008) based on the experimental test results of 11 specimens. The shear strains corresponding to the maximum and residual strengths respectively, 0.02 and 0.185 for exterior joints with transverse reinforcement, 0.016 and 0.077 for exterior joints without transverse reinforcement, 0.02 and 0.187 for interior joints with transverse reinforcement, and 0.019 and 0.117 for interior joints without transverse reinforcement. These values are adopted from Jeon (2013) based on the experimental test results of 154 specimens. Fig. 8 shows the shear stress-strain curves for exterior and interior joints with and without transverse reinforcement.

If the longitudinal reinforcement of a beam has insufficient straight embedment, a reduced shear stress-strain curve should be developed and used for that particular loading direction (e.g., upward in Fig. 8) when defining the rotational spring. These curves are shown with red lines in Fig. 8, where the bond strength ($v_{bond}$) is computed in terms of the shear strength proposed by Hassan (2011). The input parameters required to compute $v_{bond}$ are the concrete compressive strength ($f'_c$), the reinforcement factor which is dependent on the beam longitudinal reinforcement diameter ($\varphi_b$) and concrete cover ($cc$), the axial load factor (ALF), the tension force in the beam longitudinal reinforcement ($T$), and the embedment length ($l_s$) of the beam reinforcement within joint. Once $v_{bond}$ is computed, the shear stress-strain curve with bond slip is defined as shown in Fig. 8 with red lines where the yield and residual strengths are 95% and 20% of $v_{bond}$, respectively. The developed spreadsheet (Suwal and Guner 2023a) executes these calculations and provides the values required for the construction of the shear stress-strain curves.

To define a rotational spring in a global frame analysis, the calculated shear stress-strain points should be transformed into equivalent moment-rotation points. For this, the modeling approach uses the formulations proposed by Celik and Ellingwood (2008) as shown below.

$$M_{max} = v_{max} \; A_j \frac{1}{\frac{1-h_c/L_b}{jh_{be}} - \frac{\alpha}{L_c}} \tag{1}$$

$$M_{bond} = v_{bond} A_j \frac{1}{\frac{1-h_c/L_b}{jh_{be}} - \frac{\alpha}{L_c}} \tag{2}$$

$$\theta = \gamma \tag{3}$$

$M_{max}$ *and* $M_{bond}$ are the equivalent moment capacities for shear and bond strengths, respectively, $h_{be}$ is the effective depth of the beam (to the centroid of the reinforcement), $A_j$ is the area of the joint core ($A_j = h_b \times h_c$), $j$ is a constant taken as 0.875, and $\alpha$ is a constant equal to 2 for knee joints and 1 for all other joints. Since the joint rotation is the change in the angle between the two edges of the joint core, the rotation is equivalent to the shear strain as shown in Eq. (3). Using these equations, the equivalent moment-rotation curves for various joint and reinforcement anchorage conditions are shown in Fig. 9. The developed spreadsheet (Suwal and Guner 2023a) executes these calculations and provides the moment-rotation points for inputting into a global frame analysis when defining rotational hinge.

To model a beam-column joint using Model 2, two types of springs are defined as plastic hinges: a shear spring in the column region and a rotational spring in the beam region (see Fig. 10). The shear spring models the shear deformation while the rotational spring models the bond slip behavior.

Analogous to Model 1, four points should be defined to develop the shear stress-strain and moment-rotation curves required for the shear and rotation spring hinges,

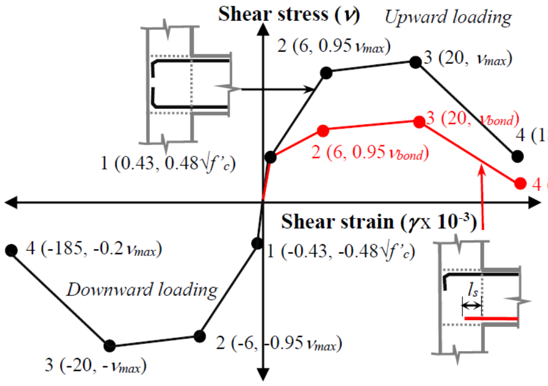


(a) Exterior joint with transverse reinforcement

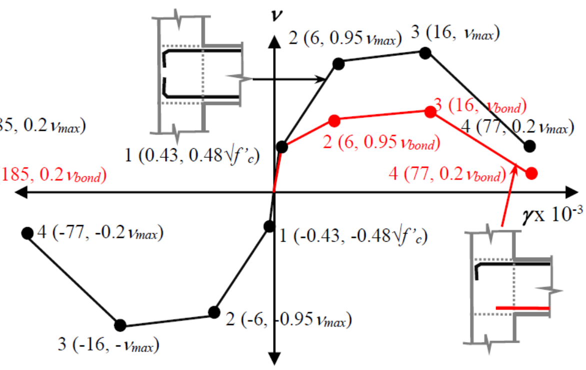


(b) Exterior joint without transverse reinforcement

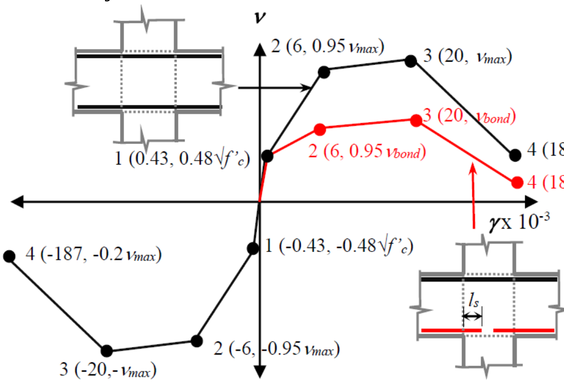


(c) Interior joint with transverse reinforcement

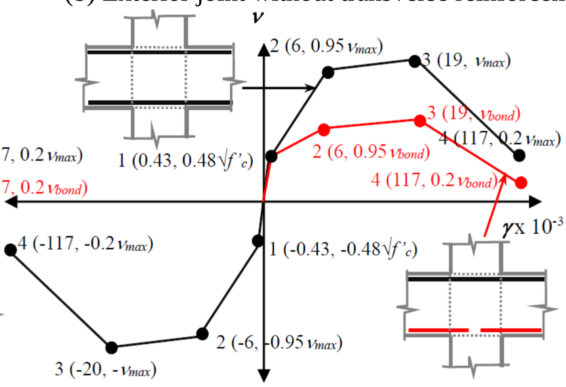


(d) Interior joint without transverse reinforcement

Fig. 8 Shear stress-strain curve developed using Model 1 (adopted from Jeon 2013)

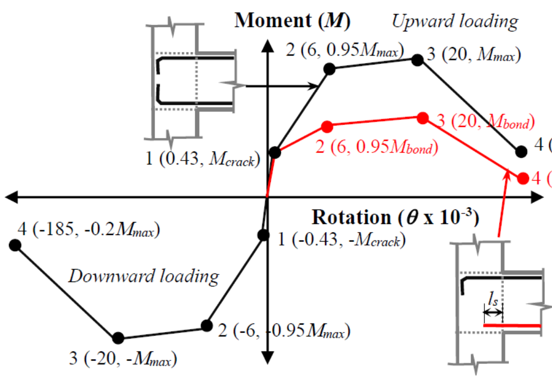


(a) Exterior joint with transverse reinforcement

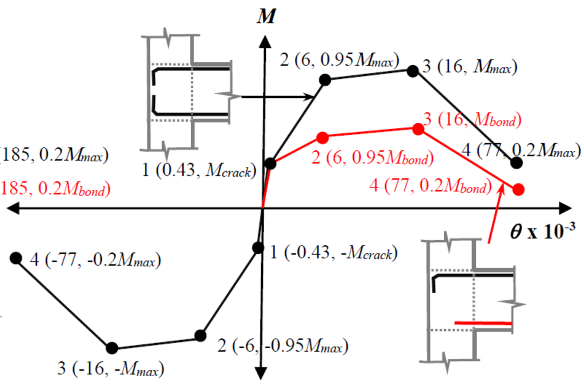


(b) Exterior joint without transverse reinforcement

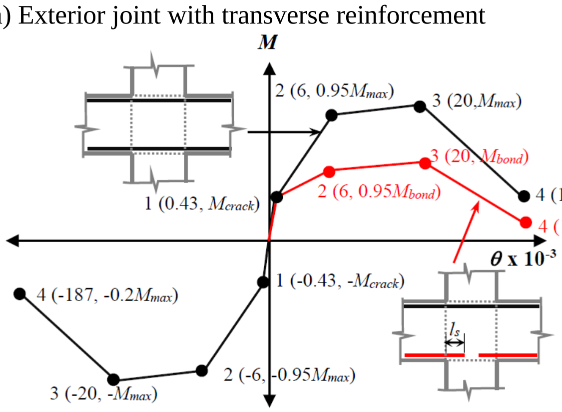


(c) Interior joint with transverse reinforcement

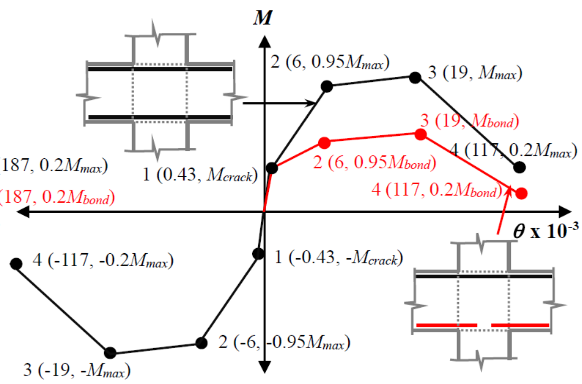


(d) Interior joint without transverse reinforcement

Fig. 9 Moment-rotation curve developed using Model 1 ( adopted from Jeon 2013)

respectively. The input parameters required to define the shear strength and moment capacity are the concrete

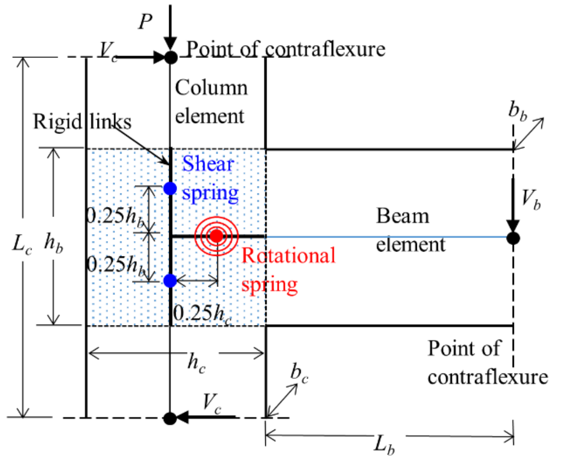


Fig. 10 Location of spring elements in exterior joint using Model 2

compressive strength ($f'_c$), the cross-sectional dimensions of the beams and columns ($b_b$, $b_c$, $h_b$, $h_c$), the clear length of the beam from the face of the column to the point of contraflexure ($L_b$), the column length between two points of contraflexure ($L_c$), the axial stress in the column $\sigma_a = P/(h_c \times b_c)$, the principal tensile stress ($p_t$), and the tensile force in the beam longitudinal reinforcement ($T$). This model uses a failure criterion based on limiting principal tensile stresses in the joint core; therefore, the curves are developed by computing the shear and moment capacities at different principal tensile stress levels. For exterior joints with properly hooked reinforcing bars, the principal tensile stress for cracking is defined as $0.29\sqrt{f'_c}$, yielding and maximum as $0.42\sqrt{f'_c}$, and residual as $0.10\sqrt{f'_c}$, based on Priestley (1997). For exterior joints with insufficient straight embedment of beam longitudinal reinforcement, the principal tensile stress for cracking is defined as $0.13\sqrt{f'_c}$, both yielding and maximum as $0.19\sqrt{f'_c}$, and residual as $0.06\sqrt{f'_c}$, based on Murty *et al.* (2003). Once the principal tensile stresses are defined, the shear stress and moments values corresponding to cracking, yielding, maximum, and residual are computed. In Fig. 11, the shear stress and moment values for cracking are $v_{crack}$ and $M_{crack}$, yielding are $v_{yield}$ and $M_{yield}$, maximum are $v_{max}$ and $M_{max}$, and residual are $v_{resid}$ and $M_{resid}$, respectively. Similarly, the shear strains and rotations corresponding to cracking, yielding, maximum, and residual are defined as 0.0002, 0.002, 0.005, and 0.025, respectively for joints with properly hooked reinforcing bars, and 0.0002, 0.002, 0.005, and 0.015, respectively for joints with insufficient straight embedment of beam longitudinal reinforcement. The resulting shear stress-strain and moment-rotation curves are shown in Figs. 11(a) and 11(b), respectively. These values are used as input in a global frame analysis when defining the shear and rotational hinges. The developed spreadsheet (Suwal and Guner 2023a) calculates both curves, as per the calculation process defined in Sharma *et al.* (2011) and provides four pairs of data for copying and pasting into frame analysis software.

The third stage involves the derivation and placement of moment and shear hinges to model the inelastic behavior of

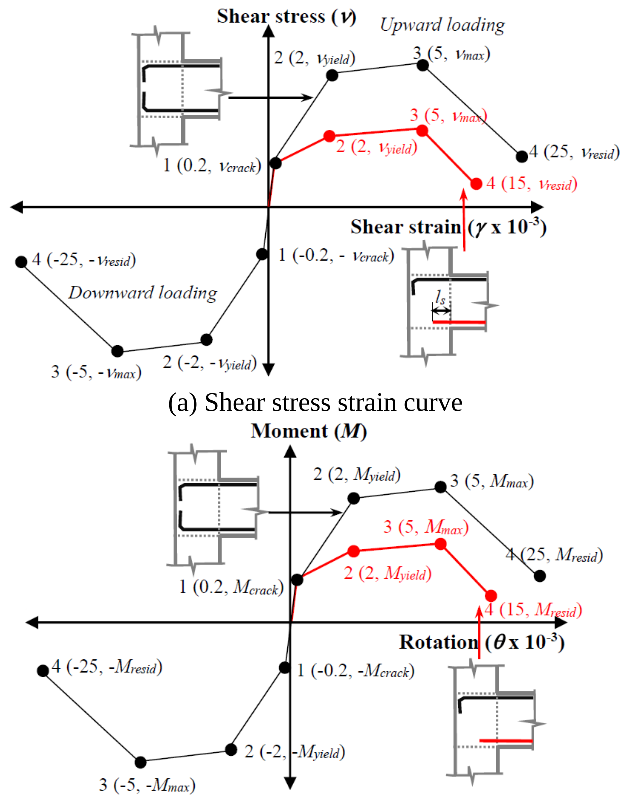


(a) Shear stress strain curve

(b) Moment rotation curve

Fig. 11 Shear stress-strain and moment-rotation curve developed using Model 2 (adopted from Sharma *et al.* 2011)

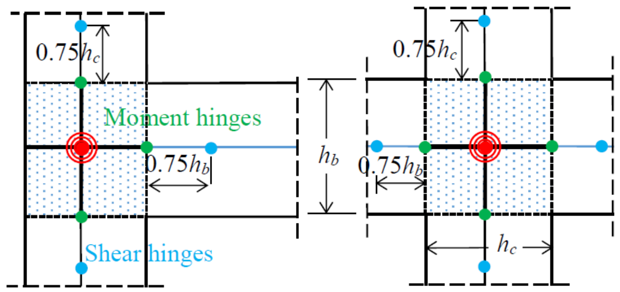


(a) Exterior joint (b) Interior joint

Fig. 12 Beam, column and joint modeling using Model 1

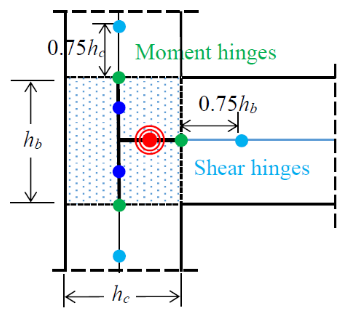


Fig. 13 Beam, column and joint modeling using Model 2

beams and columns at the hinge locations. This is a common stage undertaken in plastic-hinge-based frame analysis and therefore only critical aspects are discussed.

The moment hinge is assigned at the interface of the beams and columns (see Figs. 12 and 13) due to the peak values taking place at these points. The hinge length for the moment hinge is commonly taken as the cross-section depth ($h_b$ ) which is also recommended in CSI (2016). The shear hinge is defined $0.75h_b$ away from the interface with a depth of $1.5h_b$ (Guner 2008). A schematical overview of the hinge locations for beams, columns, and beam-column joints using either Models 1 or Model 2 is shown in Fig. 12 and Fig. 13 respectively.

The fourth stage involves the application of the loads. This is common across various frame analysis methods. The loads could be applied in a force or displacement-controlled manner depending on the pushover analysis method used.

The final stage is to run the analysis and calculate the hinge conditions for each load stage. Common frame analysis software, such as SAP2000 (CSI 2016), ETABS (CSI 2016), RISA-3D (RTI 2020), MIDAS Civil (MI 2021), PERFROM-3D (CSI 2011) may be used. Some of the software provide color-coded hinge conditions which enables the identification of the hinge condition from point 1 to 4 (See Fig. 9 and Fig. 11) to determine the governing behavior and failure mode.

## 4. Application and experimental validation of the proposed approach

The objective of this section is to demonstrate the application and experimental validation of the proposed modelling approach. It should be noted that the theoretical formulation of Model 1 was previously validated with the experimental tests of 28 interior and exterior joint specimens with errors up to 8.4% (Jeon 2013), and Model 2 with 12 exterior joint specimens with an average error of 8.6% (Sharma *et al.* 2011). For demonstration purposes, an exterior joint specimen from the literature is modelled with the proposed approach and the predicted responses are compared with the experimental results. The modelled experimental specimen is shown in Fig. 14. The compressive strength of the concrete is 33.1 MPa. The column has 25M reinforcing bars with 10M hoops while the beam has 29M bars and 10M stirrups. The yield strength ($f_y$) and ultimate strength ($f_u$) of the reinforcement are 459 and 761 MPa for 29M bars, 470 and 742 MPa for 25M bars, and 427 and 654 MPa for 10M bars, respectively. The top longitudinal reinforcement of the beam was bent into the joint, whereas the bottom reinforcement was extended straight 152 mm from the face of the column. The axial load applied to the column was 10% of the concrete compressive strength and the test setup used pin supports at the top and bottom of column. The beam and column have sufficient reinforcement (longitudinal and transverse) to prevent early beam and column damage while there is no transverse reinforcement in the joint to confine the core. Therefore, this is a well-suited specimen to validate beam-column joint modeling approaches.

The proposed approach requires the use of either Model 1 or Model 2. However, for demonstration and validation purposes, both models are employed as presented below.

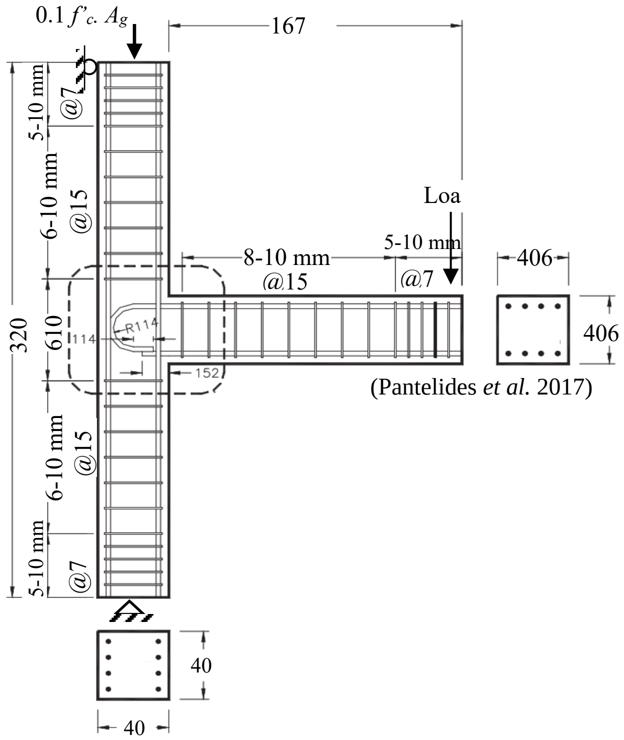


Fig. 14 Experimental setup of the specimen modelled

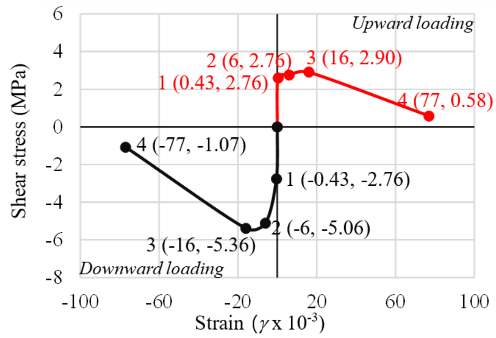


(a) Shear stress-strain curve

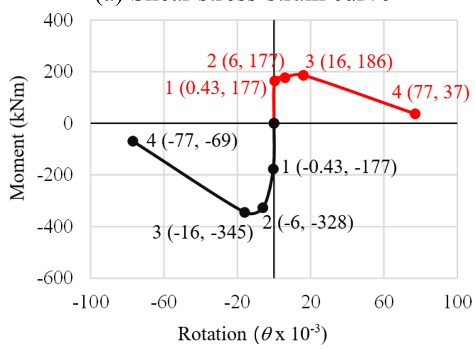


(b) Moment-rotation curve

Fig. 15 Shear stress-strain and moment-rotation curves obtained using Model 1

### *4.1 Using joint model 1*

The procedure discussed in Section 3 is applied to this specimen. A rotational spring element is defined as the plastic hinge in the joint as shown in Fig. 7. This rotational

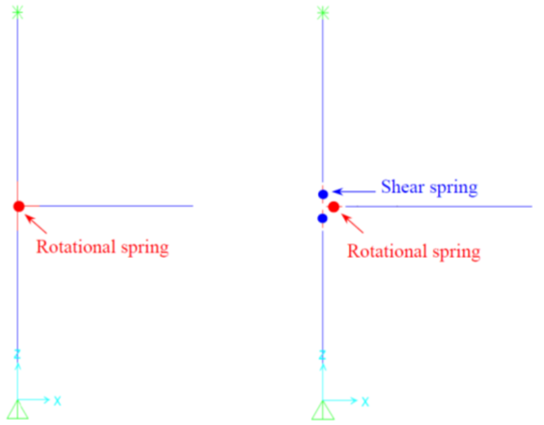


(a) Model 1 (b) Model 2

Fig. 16 Frame models developed with joint hinges

spring represents shear and bond slip behaviors. The joint shear stress-strain, and moment-rotation curves are derived with the help of the developed spreadsheet and presented in Fig. 15. The shear strengths in the upward and downward loading directions are calculated as 2.90 MPa and -5.36 MPa, respectively, and the moment capacities in the upward and downward loading directions are calculated as 186 kNm and -345 kNm, respectively. These values are then used in the global frame analysis software to define the plastic hinges shown in Fig. 16(a).

### *4.2 Using joint model 2*

The procedure discussed in Section 3 is applied to this specimen. Two types of spring elements are required by this model. A shear spring hinge is used to model shear deformation while a moment spring hinge is used to model the bond slip effect as shown in Fig. 10. The joint shear stress-strain, and moment rotation curves are derived with the help of developed spreadsheet and presented in Fig. 17.

The shear strengths in the upward and downward loading directions are computed as 0.40 MPa and -0.74 MPa, respectively, and the moment capacities in the upward and downward loading directions are computed as 194 kNm and -354 kNm, respectively. These values are used as the spring characteristics in the global frame analysis software to model the joint's behavior. These values are then used in the global frame analysis software to define the plastic hinges shown in Fig. 16(b).

### *4.3 Defining beam and column hinges*

In the third stage, plastic hinges for shear and moment are derived and placed at the critical location of the frame elements as discussed in Section 3. Figs. 18(a) and (b) show the location of all plastic hinges (for both frame elements and joint) using both joint models. These are the final frame models used in this validation study.

### *4.4 Applying the loads and performing the analysis*

In the fourth stage, a constant axial load of 542 kN is applied at the column. A displacement-controlled pushover analysis protocol is used for the load application at the tip of the cantilever beam. In the fifth stage, the analysis is run until the failure of the specimen.

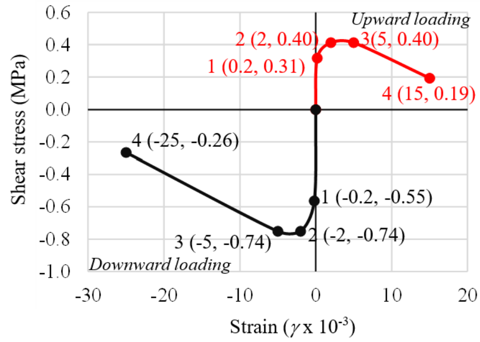


(a) Shear stress-strain curve for the shear spring

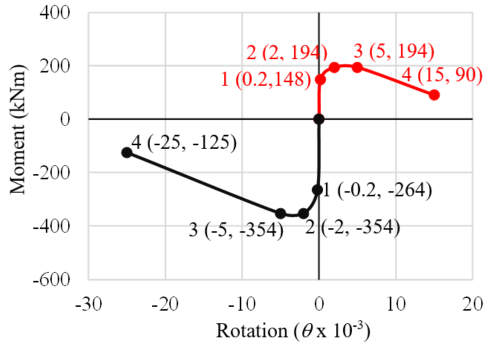


(b) Moment-rotation curve for the rotational spring

Fig. 17 Shear stress-strain and moment-rotation curves obtained using Model 2

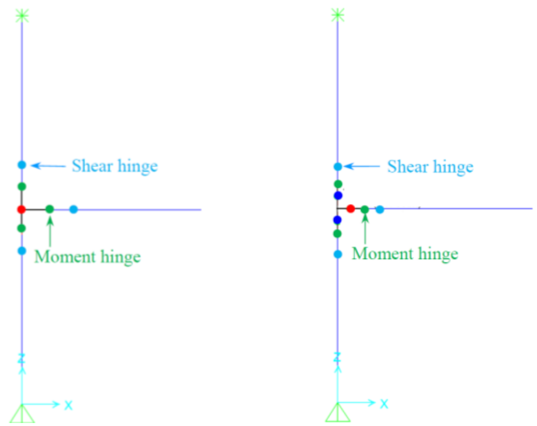


(a) Model 1 (b) Model 2

Fig. 18 Frame models developed with all hinges

### *4.5 Comparison of predicted and experimental results*

Fig. 19 shows the progression of the joint damage under increased beam loading in the experimental study. Level I corresponds to the first yielding of the longitudinal reinforcement, Level II to the formation of the bond slip mechanism, Level III to significant shear cracking in the joint core, Level IV to significant spalling of concrete at joint interface, and Level V is the loss of the load capacity.

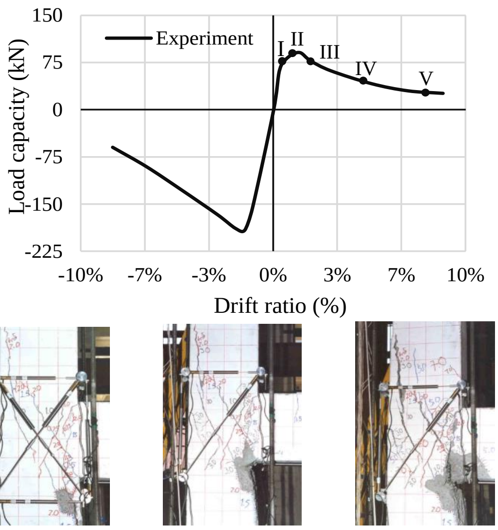


Level III Level IV Level V

Fig. 19 Joint damage progression (Pantelides *et al.* 2002)

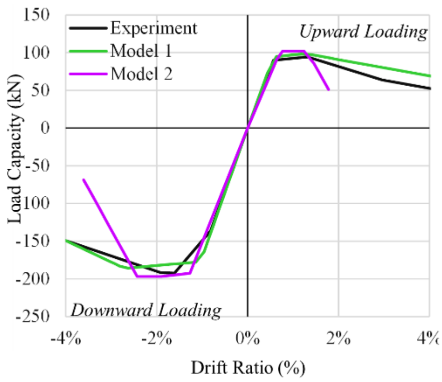


Fig. 20 Comparison of the analysis results with the experimental result

Fig. 20 shows the comparison of the analysis results (using the proposed modeling approach) with the experimental results. Both models performed numerically efficiently and provided accurate responses.

Model 1 captured the experimental load capacity reasonably well. The ratio of the predicted load ($P_p$) to the experimental load ($P_{exp}$) is 0.96 and 1.04 for the downward and upward loading directions, respectively. This specimen exhibited a bond slip failure in the upward loading direction while a joint shear failure in the downward loading direction. The failure modes in both directions are predicted accurately by the analysis. The average calculation error is 4.2% which is considerably less than the error one could expect to have when modeling shear and bond slip behaviors.

Model 2 also captured the experiment response reasonably well. The ratio of the predicted load ($P_p$) to the experimental load ($P_{exp}$) is 1.02 and 1.08 for the downward and upward loading directions, respectively. The average calculation error is 5.0% which is also well acceptable. Model 2 was also able to capture the failure modes in both loading directions accurately.

The post-peak response of joints sustaining shear and

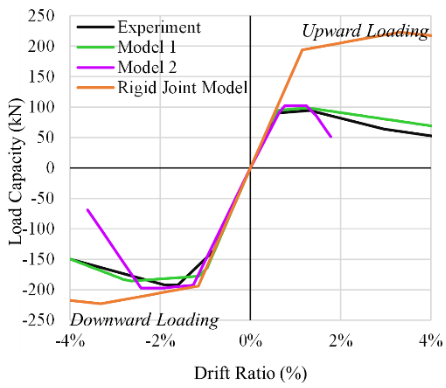


Fig. 21 Comparison of the analysis results with the experimental result

Table 1 Comparison of predicted and experimental results

| | Downward loading (kN) | $P_p/P_{exp}$ | Upward loading (kN) | $P_p/P_{exp}$ |
|---|---|---|---|---|
| Experiment | 192.6 | 1.00 | 94.3 | 1.00 |
| Model 1 | 185.6 | 0.96 | 98.1 | 1.04 |
| Model 2 | 196.9 | 1.02 | 102.1 | 1.08 |
| Rigid Joint Model | 220.7 | 1.15 | 220.7 | 2.34 |

bond-slip failures are more challenging to capture and typically requires more sophisticated modeling approaches, such as component or finite element models. This is also evident from the predicted post-peak responses which show deviations from the experimental responses. The rotational spring models are most useful for the calculation of load and deformation responses up to the peak load on which the design or assessment should be based in forensic engineering studies.

To demonstrate the significance of modeling the shear and bond-slip behaviors in joints, the same specimen is modelled using a rigid joint model. This approach only uses rigid links in the joint core without any rotational or shear springs. This neglects the deformations in the joints and enforces the assumption that the beam and column members remain perpendicular even under significant deformations. Fig. 21 shows the comparison of the predicted results. The ratio of the predicted load ($P_p$) to the experimental load ($P_{exp}$) is 1.15 and 2.34 for the downward and upward loading directions, respectively. The omission of the bond slip failure in the upward loading direction resulted in a major discrepancy with the experimental results. If this modeling approach was used for the analysis, a highly inaccurate and unsafe prediction would have been obtained. Table 1 summarizes the responses obtained for this specimen from three modeling approaches.

## 5. Conclusions

This study presented a beam-column joint modeling approach based on mathematical formulations available in the literature to aid practicing engineers in incorporating joint modeling into global frame analysis using 1D frame elements. The proposed approach integrates rotational spring models into lumped-plasticity-based frame analysis methods based on two distinct formulations. A spreadsheet tool is also developed to execute the mathematical calculations. The modeling approach, and the spreadsheet, is verified by modeling of an exterior joint from the literature through a global frame analysis. The predicted responses are compared with the experimental results. The findings of the study support the following conclusions:

- Beam-column joints are susceptible to exhibiting shear and bond-slip failure modes. It is important to include both modes in global frame models for forensic studies. The rigid joint models omit both behaviors and may provide highly inaccurate and unsafe response predictions for joints exhibiting shear and/or bond slip behaviors.
- Rotational spring models provide a good balance between the simplicity and accuracy for the forensic analysis of frames. They are particularly useful for predicting the response up to the peak load capacity.
- The proposed modeling approach is numerically efficient and practical. It can be implemented into global frame analysis software when defining plastic hinges.
- The developed spreadsheet facilitates the derivation of the hinge curves and generates the data needed for inputting into global frame analysis software.
- The experimental validation study demonstrates that the proposed modeling approach captures both joint shear and bond slip failure models and predicts the beam-column joint capacity with a maximum error of 8.0% for the specimen investigated in this study.
- Model 1 is applicable to a wide range of joint types including interior and exterior joints with and without transverse reinforcement. The shear and bond slip behaviors are modelled with a single rotational spring. Joint Model 2 is limited to the exterior joints without transverse reinforcement. The shear and bond slip behaviors are modelled with shear and rotational springs to separately. This may provide advantages if discrete consideration of shear and bond slip behaviors is desired.
- The proposed modeling approach is not limited to joint Model 1 and Model 2. Any other validated rotational spring models may also be used.

## Acknowledgments

The author would like to thank Mr. Prajwol Hada, a graduate student in the Department of Civil and Environmental Engineering at the University of Toledo, for his help with creating the figures and editing the references list.

## References

Abusafaqa, F.R., Samaaneh, M.A. and Dwaikat, M.B.M. (2022), “Improving ductility behavior of sway-special exterior beam-column joint using ultra-high-performance fiber-reinforced concrete”, *Struct.*, **36**(12), 979-996. https://doi.org/10.1016/j.istruc.2021.12.059.

Alagundi, S. and Palanisamy, T. (2022), “Neural network prediction of joint shear strength of exterior beam-column joint”, *Struct.*, **37,** 1002-1018. https://doi.org/10.1016/j.istruc.2022.01.013.

Alath, S. and Kunnath, S.K. (1995), “Modeling inelastic shear deformations in RC beam-column joints”, *Proceedings of 10th Conference*, Boulder, CO, USA.

Alwanas, A.A.H., Al-Musawi, A.A, Salih, S.Q., Tao, H., Ali, M. and Yaseen, Z.M. (2019), “Load-carrying capacity and mode failure simulation of beam-column joint connection: Application of self-tuning machine leaning model”, *Eng. Struct.*, **194,** 220-229. https://doi.org/10.1016/j.engstruct.2019.05.048.

Anderson, M., Lehman, D. and Stanton, J. (2008), “A cyclic shear stress-strain model for joints without transverse reinforcement”, *Eng. Struct.*, **30**(4), 941-954. https://doi.org/10.1016/j.engstruct.2007.02.005.

Biddah, A. and Ghobarah, A. (1999), “Modelling of shear deformation and bond slip in reinforced concrete joints”, *Struct. Eng. Mech.*, **7**(4), 413-32. https://doi.org/10.12989/sem.1999.7.4.413.

Birely, A.C., Lowes, L.N. and Lehman, D.E. (2012), “A model for the practical nonlinear analysis of reinforced-concrete frames including joint flexibility”, *Eng. Struct.*, **34**(1), 455-465. https://doi.org/10.1016/-j.engstruct.2011.09.003.

Celik, O.C. and Ellingwood, B.R. (2008), “Modeling beam-column joints in fragility assessment of gravity load designed reinforced concrete frames”, *J. Earthq. Eng.*, **12**(3), 357-381. https://doi.org/-10.1080/13632460701457215.

Clyde, C., Pantelides, C.P. and Reavely, L.D. (2000), “Performance-based evaluation of exterior reinforced concrete building joints for seismic excitation”, PEER Report 2000; Pacific Earthquake Engineering Research Center, College of Engineering, University of California, Berkeley, CA, USA.

Computers and Structures, Inc. (2011), PERFORM-3D™ - Nonlinear Analysis and Performance Assessment for 3D Structures User’s Guide Version 5, Computers and Structures, Inc., Berkeley, CA, USA.

Computers and Structures, Inc. (2016), ETABS - Integrated Building Design Software User’s Guide, Computers and Structures Inc., Berkeley, CA, USA.

Computers and Structures, Inc. (2016), SAP2000 - Integrated Software for Structural Analysis and Design User’s Manual Version 19, Computers and Structures, Inc., Berkeley, CA, USA.

De Risi, M.T., Ricci, P. and Verderame, G. (2017), “Modelling exterior unreinforced beam-column joints in seismic analysis of non-ductile RC frames”, *Earthq. Eng. Struct. Dyn.*, **46**(6), 899-923. https://doi.org/10.1002/eqe.2835.

Eligehausen, R., Ozbolt, J., Genesio, G., Hoehler, M.S. and Pampanin, S. (2006), “Three-dimensional modeling of poorly detailed RC frame joints”, *Proceedings of the Annual NZSEE Conference*, Napier, New Zealand.

Gao, X. and Lin, C. (2021), “Prediction model of the failure mode of beam-column joints using machine learning methods”, *Eng. Fail. Anal.*, **120**, 105072. https://doi.org/10.1016/j.engfailanal.2020.105072.

Ghobarah, A. and Said, A. (2002), “Shear strengthening of beam-column joints”, *Eng. Struct.*, **24**(7), 881-888. https://doi.org/10.1016/S0141-0296(02)00026-3.

Gombosuren, D. and Maki, T. (2020), “Prediction of joint shear deformation index of RC beam-column joints”, *Build.*, **10**(10), 176. https://doi.org/10.3390/buildings10100176.

Grande, E., Imbimbo, M., Napoli, A., Nitiffi, R. and Realfonzo, R. (2021), “A nonlinear macro-model for the analysis of monotonic and cyclic behaviour of exterior RC beam-column joints”, *J. Build. Eng.*, **39,** 16.

https://doi.org/10.1016/j.jobe.2021.102202.

Guner, S. (2008), "Performance assessment of shear-critical reinforced concrete plane frames", Ph.D. Dissertation, University of Toronto, Toronto, Canada.

Guner, S. and Vecchio, F.J. (2008), *User's manual of VecTor5*, Department of Civil Engineering, University of Toronto, Toronto, Canada.

Guner, S. and Vecchio, F.J. (2011), "Analysis of shear-critical reinforced concrete plane frame elements under cyclic loading", *J. Struct. Eng.*, **137**(8), 834-84. https://doi.org/10.1061/(ASCE)ST.1943-541X.0000346

Haido, J.H. (2022), "Prediction of the shear strength of RC beam-column joints using new ANN formulations", *Struct.*, **38**, 1191-1209. https://doi.org/10.1016/j.istruc.2022.02.046.

Hassan, W.M. (2011), "Analytical and experimental assessment of the seismic vulnerability of beam-column joints without transverse reinforcement in concrete building", Ph.D. Dissertation, University of California, Berkeley, CA, USA.

Huang, G.B., Zhu, Q.Y. and Siew, C.K. (2006), "Extreme learning machine: theory and applications", *Neurocomput.*, **70**(1), 489-501. https://doi.org/10.1016/j.neucom.2005.12.126.

Jeon, J.S. (2013), "Aftershock vulnerability assessment of damaged reinforced concrete buildings in California", Ph.D. Dissertation, Georgia Institute of Technology, Atlanta, GA, USA.

Jeon, J.S., Lowes, L.N. and DesRoches, R. (2014), "Numerical models for beam-column joints in reinforced concrete building frames", *ACI Spec. Publ.*, **6**(3), 297-323. https://doi.org/10.14359/51686900.

Kotsovou, G.M., Cotsovos, D.M. and Lagaros, N.D. (2017), "Assessment of RC exterior beam-column joints based on artificial neural networks and other methods", *Eng. Struct.*, **144**, 1-18. https://doi.org/10.1016/j.engstruct.2017.04.048.

Lowes, L.N. and Altoontash, A. (2003), "Modeling reinforced-concrete beam-column joints subjected to cyclic loading", *J. Struct. Eng.*, **129**(12), 1686-1697. https://doi.org/10.1061/(ASCE)0733-9445(2003)129:12(1686).

Mangalathu, S. and Jeon, J.S. (2018), "Classification of failure mode and prediction of shear strength for reinforced concrete beam-column joints using machine learning techniques", *Eng. Struct.*, **160**, 85-94, https://doi.org/10.1016/j.engstruct.2018.01.008.

MIDAS (2021), MIDAS CIVIL - Analysis for Civil Structures, Analysis Reference, MIDASoft, Inc., New York, NY, USA.

Mitra, N. and Lowes, L.N. (2007), "Evaluation, calibration, and verification of a reinforced concrete beam-column joint model", *J. Struct. Eng.*, **133**(1), 105-120. https://doi.org/10.1061/(ASCE)0733-9445(2007)133:1(105).

Murty, C.V.R, Rai, D., Bajpai, K.K. and Jain, S.K. (2003), "Effectiveness of reinforcement details in exterior reinforced concrete beam-column joints for earthquake resistance", *ACI Struct. J.*, **100**(2), 149-56. https://doi.org/10.14359/12478.

Naderpour, H. and Mirrashid, M. (2019), "Classification of failure modes in ductile and non-ductile concrete joints", *Eng. Fail. Anal.*, **103**, 361-375. https://doi.org/10.1016/j.engfailanal.2019.04.047.

Pan, Z., Guner, S. and Vecchio, F.J. (2017), "Modeling of interior beam-column joints for nonlinear analysis of reinforced concrete frames", *Eng. Struct.*, **142**(4), 182-191. https://doi.org/10.1016/j.engstruct.2017.03.066.

Pantelides, C.P., Hansen, J., Nadauld, J. and Reaveley, L.D. (2002), "Assessment of reinforced concrete building exterior joints with substandard details", PEER Report 2002/18; Pacific Earthquake Research Center, University of California, Berkeley, CA, USA.

Pantelides, C.P., Hansen, J., Nadauld, J. and Reaveley, L.D. (2017), "Seismic performance of reinforced concrete building exterior joints with substandard details", *Int. J. Struct. Integr. Maint.*, **2**(1), 1-11. https://doi.org/10.1080/24705314.2017.1280589.

Parisi, F. and Augenti, N. (2017), "Structural failure investigations through probabilistic nonlinear finite element analysis: Methodology and application", *Eng. Fail. Anal.*, **80**, 386-402. https://doi.org/10.1016/j.engfailanal.2017.07.004.

Park, S. (2010), "Experimental and analytical studies on old reinforced concrete buildings with seismically vulnerable beam-column joints", Ph.D. Dissertation, University of California, Berkeley, CA, USA.

Priestley, M.J.N. (1997), "Displacement based seismic assessment of reinforced concrete buildings", *J. Earthq. Eng.*, **1**(1), 157-192. https://doi.org/10.1080/13632469708962365.

RISA (2021), RISA-Rapid Interactive Structural Analysis General Reference Version 21, RISA Tech Inc., Foothill Ranch, CA, USA.

Sagbas, G., Vecchio, F.J. and Christopoulos, C. (2011), "Computational modeling of the seismic performance of beam-column subassemblies", *J. Earthq. Eng.*, **15**(4), 640-663. https://doi.org/10.1080/13632469.2010.508963.

Sasmal, S. and Nath, D. (2016), "Evaluation of performance of non-invasive upgrade strategy for beam-column sub-assemblages of poorly designed structures under seismic type loading", *Earthq. Eng. Struct. Dyn.*, **45**(11), 1817-1835. https://doi.org/10.1002/eqe.2730.

Sharma, A., Eligehausen, R. and Reddy, G.R. (2011), "A new model to simulate joint shear behavior of poorly detailed beam-column connections in RC structures under seismic load, Part I: Exterior Joints", *Eng. Struct.*, **33**(3), 1034-1051. https://doi.org/10.1016/j.engstruct.2010.12.026.

Sharma, A., Genesio, G., Reddy, G.R. and Eligehausen, R. (2009), "Nonlinear dynamic analysis using microplane model for concrete and bond slip model for prediction of behavior of non-seismically detailed RC beam-column joints", *J. Struct. Eng.*, **36**(4), 250-257.

Shin, M. and Lafave, J.M. (2004), "Modeling of cyclic joint shear deformation contributions in RC beam-column connections to overall frame behavior", *Struct. Eng. Mech.*, **18**(5), 645-669. https://doi.org/10.12989/sem.2004.18.5.645.

Suwal, N. and Guner, S. (2023a), "Beam-column joint hinge generator for shear and bond slip behaviors", Department of Civil and Environmental Engineering, University of Toledo, OH, USA.

Suwal, N. and Guner, S. (2023b), "User bulletin 10: Joint hinge generator for shear and bond slip behaviors", Department of Civil and Environmental Engineering, University of Toledo, OH, USA.

Tibshirani, R. (1996), "Regression shrinkage and selection via the lasso", *J. Royal Stat. Soc. Ser. B (Methodol.)*, **58**(1), 267-288. https://doi.org/10.1111/j.2517-6161.1996.tb02080.x.

Thai, F.T. (2022), "Machine learning for structural engineering: A state-of-the-art review", *Struct.*, **38**(4), 448-491. https://doi.org/10.1016/j.istruc.2022.02.003.

Unal, M. and Burak, B. (2012), "Joint shear strength prediction of reinforced concrete beam-to-column connections", *Struct. Eng. Mech.*, **41**(3), 421-440. https://doi.org/10.12989/sem.2012.41.3.421.

Vecchio, F.J. and Collins, M.P. (1986), "Modified compression-field theory for reinforced concrete elements subjected to shear", *J. Am. Concrete Inst.*, **83**(2), 219-231.

Vecchio, F.J. (2000), "Distributed stress model for reinforced concrete: Formulation", *J. Struct. Eng.*, **126**(8), 1070-1077. https://doi.org/10.1061/(ASCE)0733-9445(2000)126:9(1070).

Vecchio, F.J., Bentz, E.C. and Collins, M.P. (2004), "Tools for forensic analysis of concrete structures", *Comput. Concrete*, **1**(1), 1-14. https://doi.org/10.12989/cac.2004.1.1.001.

Wong, P.S., Vecchio, F.J. and Trommels, H. (2013), "VecTor2 and formworks user's manual", Technical Report, Department of Civil Engineering, University of Toronto, ON, Canada.

Wu, X., Kumar, V., Ross, Q.J., Ghosh, J., Yang, Q., Motoda, H., McLachlan, G.J., Ng, A., Liu, B., Yu, P. and Zhou, Z.H. (2008), "Top 10 algorithms in data mining", *Knowl. Inf. Syst.*, **14**(1), 1-37. https://doi.org/10.1007/s10115-007-0114-2.

Youssef, M. and Ghobarah, A. (2001), "Modelling of RC beam-column joints and structural walls", *J. Earthq. Eng.*, **5**(1), 93-111. https://doi.org/10.1080/13632460109350387.